

Research article

Metagenomic shotgun sequencing reveals the enrichment of *Salmonella* and *Mycobacterium* in larynx due to prolonged ethanol exposure

Hui-ying Huang¹, Fei-ran Li¹, Yi-fan Zhang¹, Hui-Ching Lau, Chi-Yao Hsueh^{*}, Liang Zhou^{*}, Ming Zhang^{*}

Department of Otorhinolaryngology, Eye & ENT Hospital, Fudan University, Shanghai, China



ARTICLE INFO

Keywords:

Metagenomic sequencing
Ethanol
Alcohol
Microbiota
Function
Gene
Microenvironment

ABSTRACT

The exposure of ethanol increases the risk of head and neck inflammation and tumor progression. However, limited studies have investigated the composition and functionality of laryngeal microbiota under ethanol exposure. We established an ethanol-exposed mouse model to investigate the changes in composition and function of laryngeal microbiota using Metagenomic shotgun sequencing. In the middle and late stages of the experiment, the laryngeal microbiota of mice exposed to ethanol exhibited obvious distinguishing from that of the control group on principal-coordinate analysis (PCoA) plots. Among the highly abundant species, *Salmonella enterica* and *Mycobacterium marinum* were likely to be most impacted. Our findings indicated that the exposure to ethanol significantly increased their abundance in larynxes in mice of the same age, which has been confirmed through FISH experiments. Among the species-related functions and genes, metabolism is most severely affected by ethanol. The difference was most obvious in the second month of the experiment, which may be alleviated later because the animal established tolerance. Notable enrichments concerning energy, amino acid, and carbohydrate metabolic pathways occurred during the second month under ethanol exposure. Finally, based on the correlation between species and functional variations, a network was established to investigate relationships among microbiota, functional pathways, and related genes affected by ethanol. Our data first demonstrated the continuous changes of abundance, function and their interrelationship of laryngeal microbiota under ethanol exposure by Metagenomic shotgun sequencing.

Importance: Ethanol may participate in the inflammation and tumor progression by affecting the composition of the laryngeal microbiota. Here, we applied the metagenomic shotgun sequencing instead of 16 S rRNA sequencing method to identify the laryngeal microbiota under ethanol exposure. *Salmonella enterica* and *Mycobacterium marinum* are two dominant species that may play a role in the reconstruction of the laryngeal microenvironment, as their local abundance increases following exposure to ethanol. The metabolic function is most evidently impacted, and several potential metabolic pathways could be associated with alterations in microbiota composition. These findings could help us better understand the impact of prolonged ethanol exposure on the microbial composition and functionality in the larynx.

1. Introduction

Ethanol consumption, a common addictive behavior, is a primary risk factor that contributes to tumor occurrence and poor prognosis in patients with head and neck cancers [1]. Approximately 76,900 cases of cancer were attributed to ethanol consumption in 2016, among which nearly 60% of male cases were cancers of the upper aerodigestive tract including oral cavity, pharynx and larynx [2]. Our previous study also

suggested that abnormal ethanol metabolism is closely related to the poor prognosis of patients with laryngeal squamous cell carcinoma (LSCC) [3]. According to current evidence, ethanol may exert carcinogenesis effects through multiple biological pathways, including DNA damage, nutritional deficiencies and solvent effect for other carcinogens [4,5]. However, the existing findings cannot fully elucidate the carcinogenic mechanism of ethanol, indicating that there are still other pathways that remain to be explored.

^{*} Corresponding authors.

E-mail addresses: hsuehchiyao@gmail.com (C.-Y. Hsueh), zhoulent@126.com (L. Zhou), ent_zhm@126.com (M. Zhang).

¹ Hui-ying Huang, Fei-ran Li, and Yi-fan Zhang contributed equally to this work. Author order was determined on the basis of seniority.

Laryngeal microbiota plays a vital, but still largely unexplored, role in the formation of local tumor microenvironment. Microbiota is involved in the metabolism of ethanol to acetaldehyde, a key metabolite of ethanol with carcinogenic properties [6]. But these bacteria have a limited capacity to break acetaldehyde down further into its non-harmful compound acetate [7]. It has been suggested that long-term exposure with large amounts of ethanol can lead to prolonged direct exposure of the oropharyngeal mucosa to acetaldehyde [8–11]. Furthermore, prolonged ethanol consumption may cause dysbacteriosis of the oropharynx and enhance the pathogenicity of certain commensal microorganisms, thus forming a local microenvironment conducive to the occurrence and progression of tumors [12–14]. Take one of our previous findings, for instance, ethanol can promote *Fusobacterium nucleatum*, a conditioned pathogen enriched in the larynx of patients with laryngeal squamous cell carcinoma (LSCC), in accelerating cell metastasis and invasion [15]. Given that the composition of laryngeal microbiota in patients with head and neck carcinomas, especially those who have consumed ethanol for a prolonged period, is quite different from that in healthy people, other ethanol-induced pathogenic bacteria were speculated to be associated with these diseases [16–20]. Furthermore, the interaction between microbes, as well as their function alterations induced by ethanol, can be both involved in the malignant transformative event [21]. Nevertheless, limited studies have focused on the composition and function of microbiota located in larynx after a period of ethanol exposure, let alone its variation tendency during the period.

In the present study, we established an ethanol-drinking mouse model. Metagenomic sequencing technology was used to detect the composition of the laryngeal microbiota and its potential functional changes. Tests were designed to be continuous for a continuous analysis of ethanol intake effects on the composition and function of laryngeal microbiota. A comprehensive network was further summarized, highlighting correlations among the species, their altered functions and related genes, with the purpose of identifying potential factors contributing to the poorer prognosis of LSCC under ethanol exposure.

2. Results

2.1. Effects of ethanol on laryngeal microbiota composition

The Alpha diversity metrics, including the Chao1 index, Simpson index, and Shannon index, have revealed distribution of species within each group (Fig. 1A). The species-level analysis revealed no statistically significant difference in the community richness of laryngeal communities among different groups. However, temporal fluctuations in community diversity were observed in both NC and Ethanol groups, indicating its dynamic nature over time. The results of Principal Coordinate Analysis (PCoA) further corroborate the aforementioned findings. PERMANOVA demonstrated that there were significant compositional differences in the larynx microbiota the second and third months (PERMANOVA, $P_{adj} = 0.015$ between NC 2 month and NC 3 month; PERMANOVA, $P_{adj} = 0.007$ between Ethanol 2 month and Ethanol 3 month) (Fig. 1 B, C). The disparity between the NC and Ethanol group gradually widened with the progression of experiments, indicating that ethanol exposure had an impact on the composition of laryngeal microbiota in mice (PERMANOVA, $P_{adj} = 0.039$ between NC 2 month and Ethanol 2 month; PERMANOVA, $P_{adj} = 0.008$ between NC 3 month and Ethanol 3 month) (Fig. 1 D-F). By presenting a bar chart illustrating the distribution of the top 16 species, we can gain a comprehensive understanding of the species composition in mouse larynx, thereby facilitating subsequent analysis on fluctuations in abundance among dominant species (Fig. 1 G). Given that long-term consumption of ethanol may cause systemic effects, we have recorded the body weight and liquid feed intake of mice in different treatment groups and results were put in supplement Fig. 1 A, B.

2.2. Changes and trends in laryngeal bacterial abundance induced by ethanol exposure

By comparing the relative abundance of the top 5 bacterial genera and species in the NC and Ethanol group simultaneously, we observed that ethanol exposure could enhance *Salmonella* enrichment (Fig. 2A-F). Specifically, *Salmonella enterica* emerged as the predominant species in larynx in the ethanol-exposed group at the third month, exhibiting a significantly higher abundance compared to that of the NC group ($P = 0.0215$). In order to find biomarkers with statistical differences between different groups, we used linear discriminant analysis (LDA) effect size (LEfSe) to screen out different taxa at genus and species levels between different groups based on a standard LDA value greater than four (Fig. 2G). In the subsequent analysis of dominant species and their temporal dynamics in Ethanol group, the abundances of *Salmonella enterica* ($P = 0.0493$) and *Mycobacterium marinum* ($P = 0.0092$) exhibited temporal variations (Fig. 2H). In the NC group, the monthly decrease of *Salmonella enterica* ($P = 0.0185$) is also evident (Fig. 2I). The remaining species exhibit a lack of temporal continuity. Additionally, two species of *Pseudomonas* were involved in this change. *Pseudomonas pelagia* gradually decreased with ethanol exposure, while *Pseudomonas aeruginosa*, which increased in the third month, indicating the response to ethanol can vary significantly among different species belonging to the same genus.

2.3. *Salmonella enterica* and *Mycobacterium marinum* were observed in the larynxes of mice

To further clarify the highest relative abundance of *Salmonella* and *Mycobacterium* in the larynxes of mice, Fluorescence in Situ Hybridization (FISH) was conducted to confirm their presence in tissues. Results showed that, in the third month, *Salmonella enterica* and *Mycobacterium marinum* were observed in the larynxes of mice in Ethanol groups (Fig. 3A, B).

2.4. Changes and trend of laryngeal bacterial functions caused by ethanol exposure

To investigate the changes in bacterial functions within the laryngeal microbiota regulated by ethanol exposure, the KEGG pathway enrichment analysis was performed. The most enriched function was metabolism, including energy metabolism, carbohydrate metabolism, amino acid metabolism and metabolism of other amino acids (Fig. 4A, B). KEGG analyses of pathways were performed each month on pathway level 2 (Fig. 4C-E), among which differences between groups were most pronounced in the second month. The abundance of energy and amino acid metabolism showed an obvious increase after ethanol exposure in the second month, while the abundance of translation revealed a reduction (Fig. 4D). KEGG analyses on pathway level 3 were further conducted to clarify the enrichment degree of specific pathways (Fig. 4F).

The abundances of biosynthesis of secondary metabolism, carbon metabolism, glyoxylate and dicarboxylate metabolism, tryptophan metabolism signaling pathway, significantly increased in the Ethanol group. The multi-group comparison and analyses clearly demonstrated the abundance of pathways, especially metabolic pathways, in different groups within three months (Fig. 4G). The results showed that many metabolic pathways were significantly enriched in the Ethanol group in the second month. Synthesizing the above analytical results, there is a great possibility that underlying changes in genes or enzymes have been involved in the process during the second month of the ethanol diet.

2.5. Connections between bacterial function and genes under ethanol exposure

Species and functional regression analyses indicated that Alpha

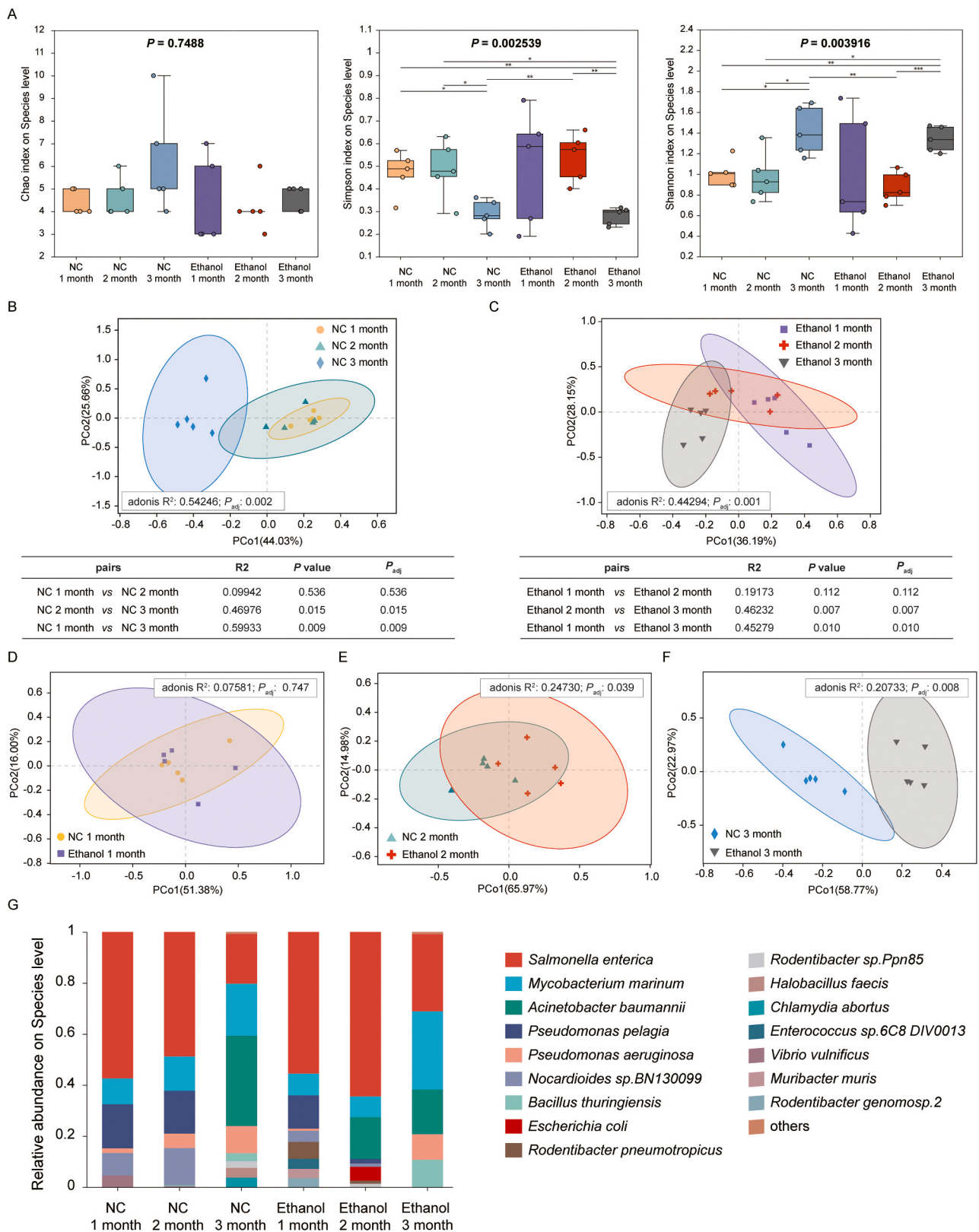


Fig. 1. Effects of ethanol exposure on the diversity and overall structure of oropharyngeal microbiota at different periods. (A) Alpha diversity indicated by Chao index, Shannon index, and Simpson index at the species level (Welch's t test, 95%, FDR). Adjusted P values are listed at the top of the bar charts. (* P < 0.05, ** P < 0.01, *** P < 0.001) (B, C) Principal coordinate analysis (PCoA) maps based on Bray-Curtis dissimilarity describe beta diversity at species level in NC and Ethanol groups. Each dot represents one sample, and the ellipse represents the 95% confidence interval (ANOSIM). (D-F) PCoA maps describe beta diversity at species level at same time point (1, 2 and 3 months) in NC and Ethanol groups (ANOSIM). (G) Bar chart of the top 16 species in six groups. Each color bar represents one species of bacteria.

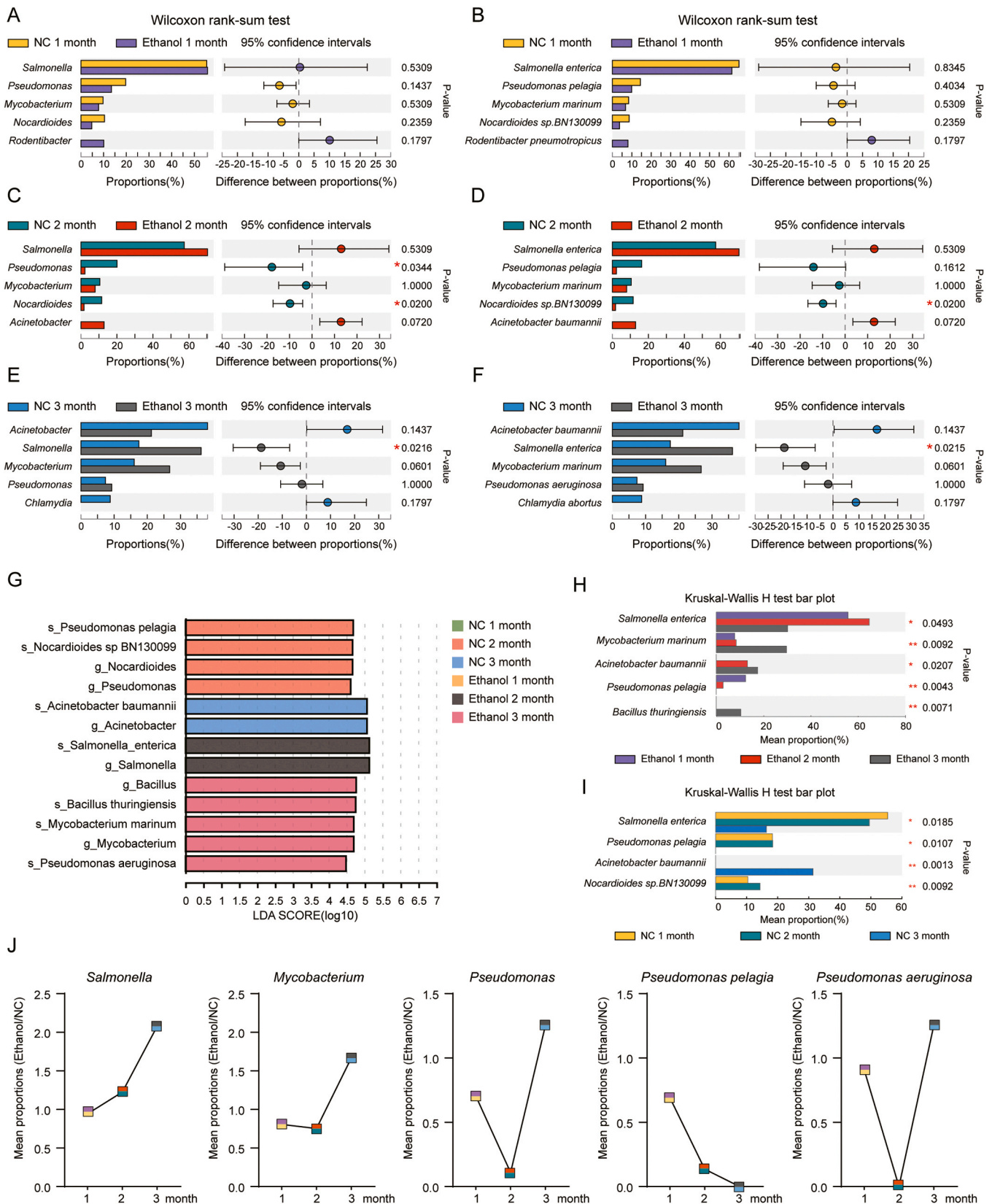


Fig. 2. Differences and the variation tendency of laryngeal microbiota composition induced by ethanol consumption. (A-F) Relative abundance of the top five bacterial genera and species between NC and Ethanol groups (Wilcoxon rank-sum test, two tail, 95%, FDR). (G) Differentially enriched taxa identified by linear discriminant analysis effect size (LEfSe) among the six groups (One-against-all). The length of the column represents the influence of significantly different species on relative abundance (LDA scores [\log_{10}] > 4). (H, I) Changes in the relative abundance of species over time in the NC and ethanol groups (Kruskal-Wallis H test, 95%, FDR, Tukey-Kramer). (J) Comparison of bacterial content and its change trend between ethanol feeding group and control group.

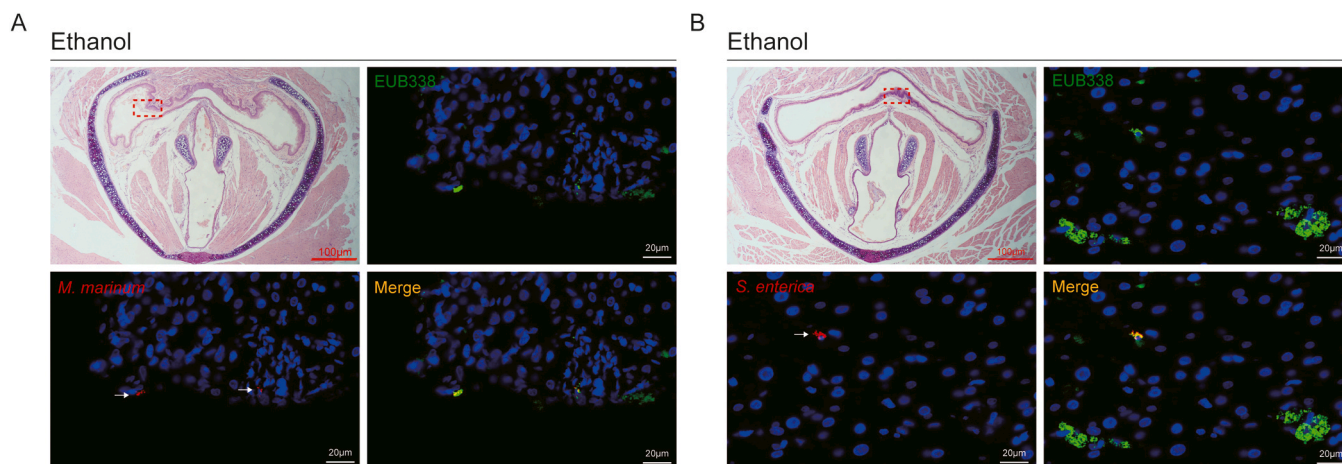


Fig. 3. FISH assays to identify *Salmonella enterica* and *Mycobacterium marinum* in the larynxes of mice. Images showing EUB338 and bacteria were cropped digitally using the SlideViewer software; bar is 20 μm and 100 μm . (A) *Mycobacterium marinum* in larynxes of mice. (B) *Salmonella enterica* in larynxes of mice.

($R2 = 0.74$) and Beta ($R2 = 0.86$) diversity of species and function were consistent with each other (Supplement figure1C, D). Analysis of the contribution capacity of different species suggested that microbiota contribute to metabolism (Fig. 5A). Take energy metabolism, for instance, microbiota in the Ethanol group contributed far more than that in the control group (Fig. 5B). The effects of *Acinetobacter baumannii* in the Ethanol group were all focused on energy metabolism (Fig. 5C). The KEGG analyses of differentially expressed genes, modules, and enzymes between NC and Ethanol groups were conducted later (Fig. 5D-F). Various modules with the highest enrichment were involved in energy metabolism (Fig. 5D). Enriched genes and enzymes were also related with metabolic pathways (Fig. 5F). Synthesizing all the above analytical results, a network was established to display the potential connection among the affected bacteria, function and KEGG pathways, KEGG modules, KEGG genes, and KEGG enzymes (Fig. 5G).

3. Discussion

Laryngeal microbiota has been identified as a key participant in the occurrence and progression of head and neck malignancies, due to variations in its basal composition and its critical role in promoting the formation of the local tumor microenvironment [12]. A link between ethanol consumption and the laryngeal microbiome has been identified in the progression of head and neck malignancies mainly through the alcohol dehydrogenase (ADH) expressed by certain bacteria species, while the exact relationship remains to be clarified [22–24]. In this study, a mouse model was constructed to explore the relationship between the composition and function variations of laryngeal microbiota under ethanol exposure, together with the potential genes that are related to bacterial function.

The laryngeal microbiota undergo significant changes due to prolonged ethanol exposure, resulting in an increased prevalence of *Salmonella enterica* and *Mycobacterium marinum*.

Previous studies suggest that persistent colonization by *Salmonella enterica* may contribute to chronic gastrointestinal inflammation and cell proliferation through modulation of the Wnt pathway, thus promoting tumorigenesis [25,26]. Additionally, effective colonization of tumors enhances the potential use of live-attenuated *Salmonella enterica* Strains as a microbial-based treatment in cancer therapy [27,28]. A recent study has demonstrated that when combined with Alb-IL2, a genetically modified strain of *Salmonella enterica* serves as an innovative therapeutic approach, inducing T cell-mediated antitumor immunity and exerting long-term tumor control in a murine model of colon cancer [29]. Therefore, apart from its potential association with local inflammation and tumorigenesis, *Salmonella enteric* may offer promising

prospects for therapeutic interventions targeting head and neck tumors in individuals with chronic alcohol consumption.

As for *Mycobacterium marinum*, a well-known pathogenic mycobacterium for skin and soft tissue infections, its abundance in the larynx was also upregulated with ethanol exposure [30]. Studies of *Mycobacterium marinum* have revealed its relationship with skin lesions including the pustular, nodular-ulcerative, granulomatous, and verrucous plaque [31, 32]. Though there is no study focusing on its effects on laryngeal diseases, considering that more than 95% of laryngeal cancers are squamous cell carcinoma (LSCC), as well as the susceptibility of the squamous epithelium to *Mycobacterium marinum*, it suggests that the formation of laryngeal tumor microenvironment and tumorigenesis may be at play. In addition, *Mycobacterium*-macrophage interaction and the resultant increase in macrophage necrosis facilitate unrestricted extracellular growth of *Mycobacterium marinum*, leading to the host being hypersusceptible and making tissues more susceptible to repeated inflammatory exposure, thus increasing the possibility of tissue malignant transformation [33,34].

Interestingly, in the alcohol exposure group, the proportion of *Pseudomonas* decreased sharply at 2 months and increased dramatically at 3 months (Fig. 2G). This phenomenon may be due to the difference in the tolerance of different *Pseudomonas* to alcohol, resulting in changes in the composition of *Pseudomonas* genus. Proportion of *Pseudomonas pelagia* gradually decreased at 2 months, while proportion of *Pseudomonas aeruginosa* significantly increased at 3 months (Fig. 2H, I). Studies have reported that ethanol can promote the enrichment of *Pseudomonas aeruginosa*, which also has a certain ability to catabolize ethanol [35,36]. Furthermore, ethanol was reported to promote *Pseudomonas aeruginosa* colonization of cystic fibrosis airway epithelial cells, which supports our findings to some extent [37]. It is worth noting that the detection results of metagenome can only reflect the relative content of bacteria, so the above results may be related to the overall abundance of microorganisms in the larynx of mice under ethanol exposure.

In terms of function, ethanol could accelerate the decay rate of enrichment degree of transcription-related pathways, indicating its inhibitory effect on laryngeal bacterial transcription. In addition, coinciding with the peak enrichment of catalase (CAT, EC 1.11.1.6), a notable enrichment of energy, amino acid, and carbohydrate metabolic pathways occurred in the second month in the Ethanol group, but fell back later in levels. As a key enzyme in the metabolism of H_2O_2 , CAT can reduce the by-products of ethanol metabolism and improve the activities of alcohol dehydrogenase (ADH), thus scavenging free radicals and protecting cells against oxidative damage [38]. CAT may also have additional roles such as anti-tumor compounds. Studies have shown a change in catalase expression in cancer cells is related to cellular

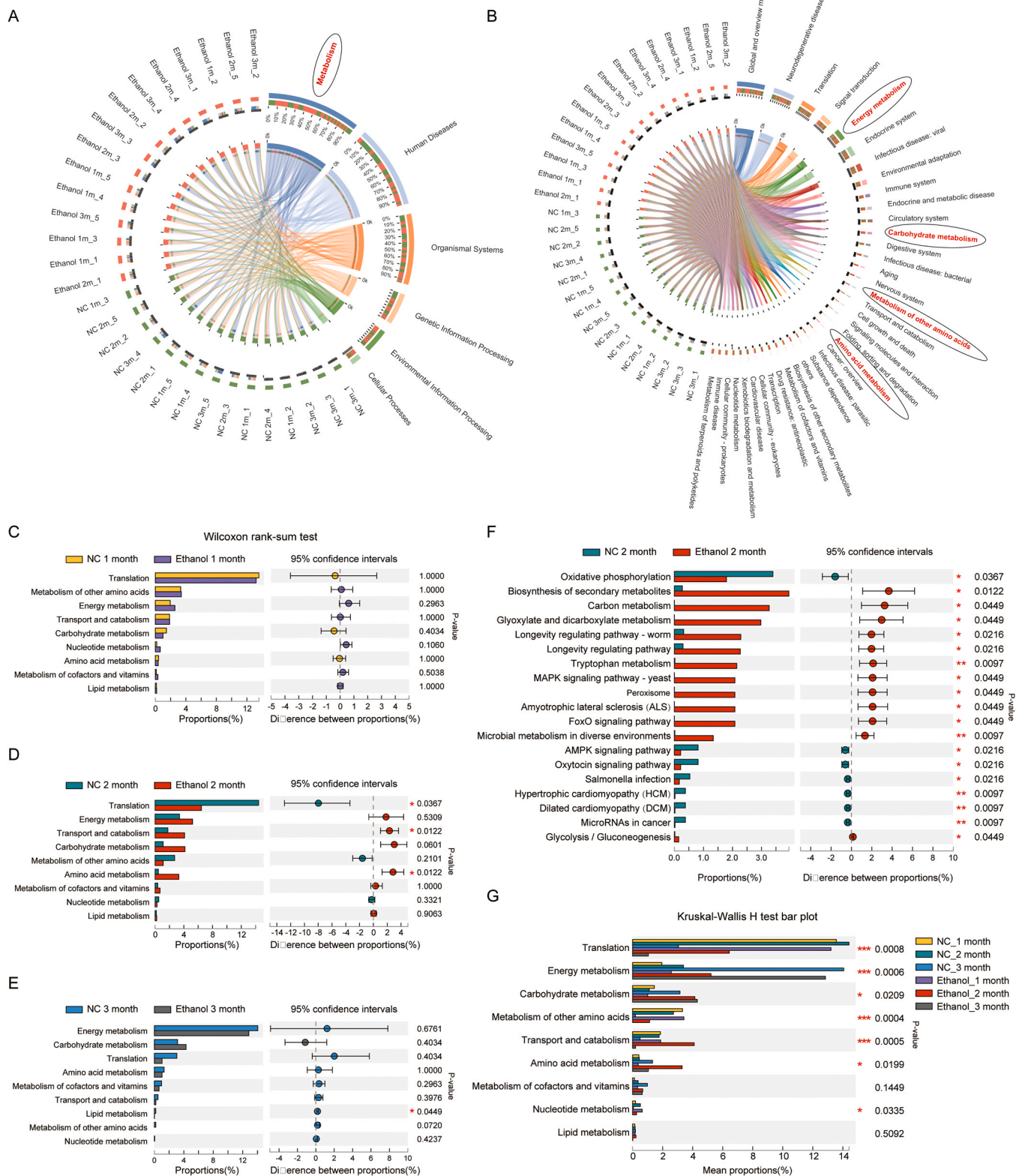


Fig. 4. Differences and the variation tendency of oropharyngeal microbiota functions induced by ethanol consumption. (A, B) Circos diagram of the KEGG pathways enrichment analysis, the left half circle represents the function abundance composition of the group, and the right half circle represents the distribution ratio of the function. (C-G) Relative abundance of KEGG pathways between the NC and Ethanol group (Wilcoxon rank-sum test, 95%, FDR, Tukey-Kramer; Kruskal-Wallis H test, 95%, FDR, Tukey-Kramer). (H) Comparison of bacterial content and its change trend between ethanol feeding group and control group.

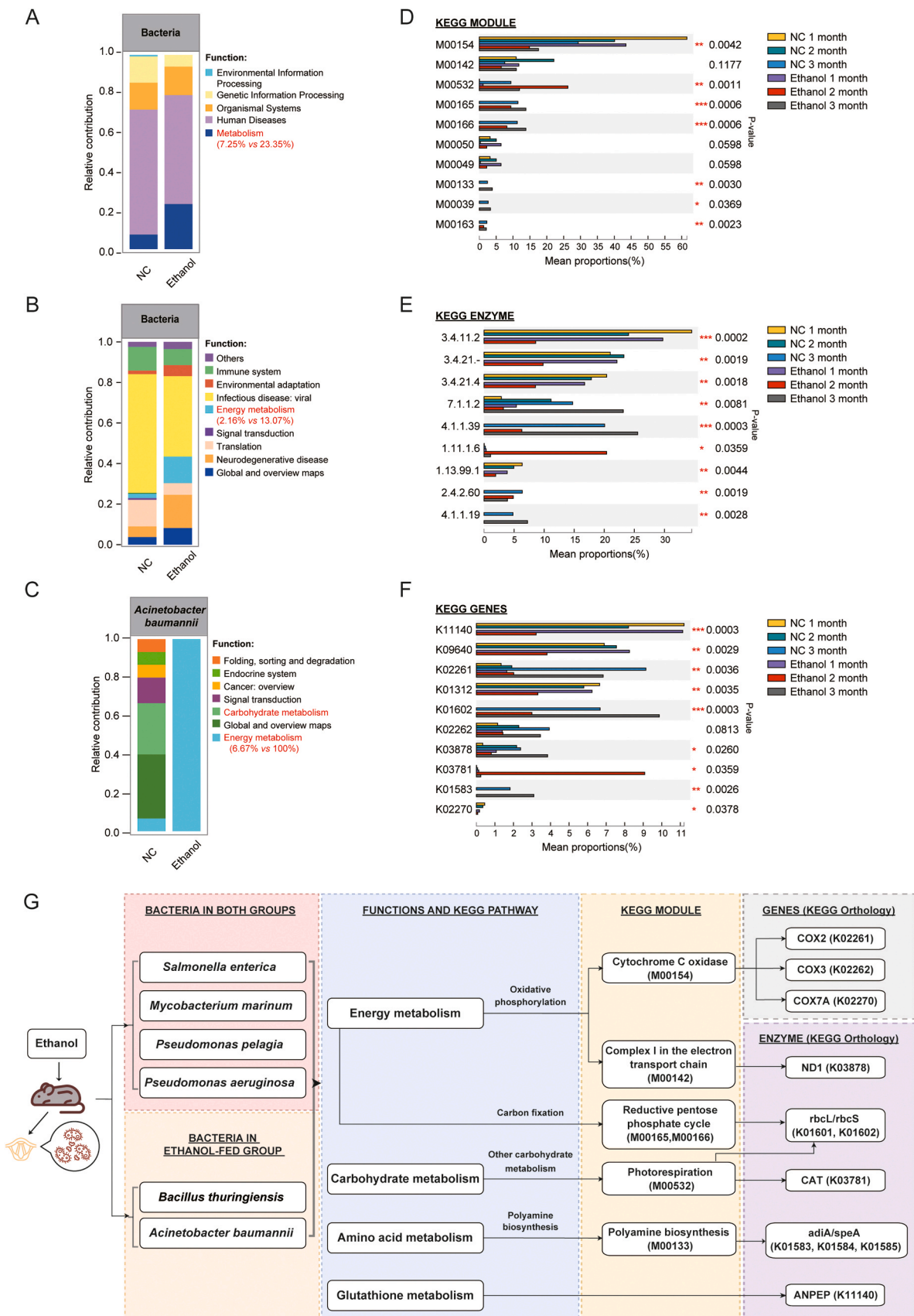


Fig. 5. Summary of the underlying connection between the affected microbes, their altered functions and several potentially related genes under ethanol exposure. (A-C) Bar plot of species and functional contribution analysis indicates the dominant species composition of a particular function. (D-F) Relative abundance of KEGG modules, enzymes and genes between the NC and Ethanol groups (Kruskal-Wallis H test, 95%, FDR, Tukey-Kramer). (G) A relationship network concerning the underlying connection between the microbes, their altered functions and several potentially related genes under ethanol exposure.

chemoresistance [39,40]. Despite the overall low amount of CAT in tumor cells, a locally high expression of CAT on the membrane of tumor cells was also found, indicating that CAT may serve as a potential target in exploring new cancer therapies [41,42]. Combined with the results of this study, in the early stage of ethanol exposure, the abundance of the catalase gene in the laryngeal flora increased, which could promote the expression of energy pathways such as carbohydrate metabolism. Though not sustained, this effect may be a kind of self-protection of bacteria under ethanol exposure and reduce the concentration of local ethanol and its metabolic by-product, H₂O₂.

Limited by the experimental time and the tolerance of mice, further investigation is required to study changes in laryngeal microbiota in mice exposed to long-term ethanol (more than six months). Although no significant differences in body weight were observed between the ethanol exposure group and the control group during the experiment, mice in the experimental group consumed significantly less food compared to those in the control group during the first two weeks. Moreover, aggression among mice escalated with prolonged ethanol intake, leading us to terminate the experiment after three months and indicating systemic effects of ethanol on mice. Since this study primarily focused on exploring changes in throat flora due to ethanol exposure, limited attention was given to overall energy metabolism and other organs of mice. It should be acknowledged that unmeasured indirect mechanisms may contribute to laryngeal dysbiosis in mice. Fortunately, species and functional regression analysis revealed associations between ethanol exposure and alterations in bacterial species functions. Consequently, genes, enzymes, modules, and pathways related to these changes were summarized.

In summary, this experiment utilized a mouse model to investigate the impact of ethanol exposure on the laryngeal microbiota. Through metagenomic sequencing, we explored the dynamic changes in both abundance and function of these microbial communities upon exposure to ethanol. Additionally, we aimed to elucidate their relationship with the formation of a microenvironment that promotes local inflammation and tumorigenesis by identifying potential bacterial genes involved in this process. By establishing a network analysis, we have summarized the key findings of our research and identified several genes that warrant further investigation. We are delighted to offer novel insights to explain the laryngeal inflammation and cancer-promoting microenvironment induced by chronic ethanol exposure from a microbial perspective.

4. Materials and methods

4.1. Animal treatment and sample collection

Six-week-old C57BL/6 mice (Shanghai Laboratory Animal Company, Shanghai, China) were housed under controlled environmental conditions (temperature 22–24 °C, relative humidity 50–60%, and 12 h light/dark cycle). All experiments involving mice were performed using protocols approved by the Animal Center at the Eye & ENT Hospital, Fudan University (No.2022076). The liquid diet used in this experiment was designed based on the AIN-93 M standard (Trophic Animal Feed High-tech Co., Ltd., China). In this experiment, 42 mice were randomly divided into 6 cages, 3 cages were randomly selected as the ethanol exposure group and the other 3 cages as the control group. Mice in the Ethanol group were administered a liquid diet containing 4% ethanol, while the NC group received a liquid feed. Although mice were in different cages, we tried to make sure they all lived in the same environment except for their diet. During the study, the liquid feed on the cage was changed daily (the remaining feed was discarded every day) and the liquid feed bottle was cleaned daily. After feeding for a period of time, mice were sacrificed using cervical vertebra dislocation on a sterile operation platform in batches. In the first and second months, we randomly selected 2 to 3 mice from each cage, bringing together 7 mice in the alcohol exposure group and 7 mice in the control group for follow-

up experiment. This method helped us avoid cage differences to some extent. The larynxes were removed, and the laryngeal tissues of two mice within each group were randomly selected and soaked in formalin solution, while the rest of the tissues from the other five mice were stored at – 80 °C until further analysis.

4.2. Fluorescence in situ hybridization (FISH)

Localizations of *Salmonella enterica* and *Mycobacterium marinum* were evaluated by FISH on 5- μ m-thick FFPE sections using a Fluorescence in Situ Hybridization Kit (RiboBio, Guangzhou, China). 16 S ribosomal RNA sequences were obtained from probeBase (<http://www.probebase.net>) and probes were synthesized by Sangon Biotech (Shanghai) Co., Ltd. The sequence of “the universal bacterial” probe was EUB338 (5'-GCTGCCTCCGTTAGGAGT-3', Alexa Fluor 488-labeled), the sequence of probe targets *Salmonella enterica* was Sal3 (5'-AATCACTTCACCTACGTG-3', Alexa Fluor 647-labeled), and the sequence of probe targets *Mycobacterium marinum* was M.marinum (5'-CGGGATT-CATGTCCTGTGGTGGAA-3', Alexa Fluor 568-labeled).

4.3. DNA isolation and metagenomic sequencing

Total genomic DNA was extracted from laryngeal tissue samples of mice using the QIAamp BioStic Bacteremia DNA Kit (Qiagen, USA) according to the manufacturer's instructions and checked by 1% agarose gel electrophoresis. The DNA was fragmented into an average size of approximately 350 bp using the Covaris M220 system (Gene Company Limited, China). A paired-end library was constructed utilizing the NEXTFLEX Rapid DNA-Seq (Bioo Scientific). Paired-end sequencing was performed on the Illumina NovaSeq 6000 platform at Majorbio Bio-Pharm Technology Co., Ltd. (Shanghai, China).

4.4. Sequence quality control, gene assembly, and prediction

The 3' end and 5' end adapter sequences were cut and low-quality reads (length <50 bp or with an average mass value <20 or having N bases) were removed using fastp software (<https://github.com/OpenGene/fastp>, version 0.20.0). The preprocessed reads were mapped to the reference *Mus musculus* genome (GRCm39) using BWA software (<http://bio-bwa.sourceforge.net/>, version 0.7.17), and any contaminated reads exhibiting high similarity were removed. Within the metagenomic data after the above screening, contigs with lengths at or above 300 bp were selected for further assembly by Megahit (<https://github.com/voutcn/megahit>, version 1.1.2) [43]. The outcomes of gene assembly can be observed in supplement table 1. The contig length distribution for each sample is depicted in supplement Figs. 2 and 3. Open reading frames (ORFs) from each assembled contig were predicted using MetaGene (<http://metagene.cb.k.u-tokyo.ac.jp/>) [44]. The predicted ORFs (no less than 100 bp) were retrieved and translated into amino acid sequences.

4.5. Gene catalog establishment and abundance calculation

To explore the commonalities and differences between different samples, CD-HIT software (<http://weizhongli-lab.org/cd-hit/>, version 4.6.1) was used to cluster the gene sequences and generate the non-redundant gene catalog with 90% sequence identity and 90% coverage [45]. Using the SOAPaligner software (<https://github.com/ShujiaHuang/SOAPaligner>, soap 2.21 release), high-quality reads of each sample were compared with non-redundant genes catalog (95% identity) to count the abundance information of genes in corresponding samples [46].

4.6. Species and functional annotation

The BLASTP tool [47] (v 2.2.28 +, <http://blast.ncbi.nlm.nih.gov/Bla>

st.cgi) was utilized to eliminate redundant gene sets and compare them against the NR database (08/2022) and KEGG gene database (v 89.1), with a BLAST alignment parameter setting an expectation value of 1e-5. Taxonomy information from the NR library was then used to annotate species comments accordingly. Subsequently, the abundances of each species were calculated by summing up their corresponding gene abundances. The abundance profiles at various taxonomic levels including Domain, Kingdom, Phylum, Class, Order, Family, Genus, and species were constructed. The KEGG Orthology Based Annotation System (KOBAS 2.0) [48] was utilized for function annotation, enabling the calculation of function category abundance by summing the gene abundances corresponding to KO, Pathway, EC, and Module.

4.7. Statistical analysis

Data were expressed as mean \pm SEM and analyzed with SPSS 22.0. For samples that were normally distributed, Student's t-test or Welch's t-test were used to evaluate the differences between the two groups. For those that were not normally distributed, Wilcoxon rank-sum test was used to seek significant differences. When investigating three or above groups, one-way ANOVA with Bonferroni's multiple comparison test was applied.

Alpha diversity was calculated by Chao, Simpson and Shannon index, based on filtered and normalized counts with rarefying to the lowest taxonomy using the vegan v2.5.6 R package. The beta diversity was calculated by principal coordinates analysis (PCoA), using Bray-Curtis dissimilarity and visualized using ggplot2 packages. PERMANOVA of the cohorts was performed using the adonis function of the vegan package in R software with permutations of 999 and Bray-Curtis dissimilarity. Microbiota functions were predicted using PICRUST2 (<https://github.com/picrust/picrust2>). The Reads Per Kilobase Million (RPKM) and relative Reads Number method were utilized to compute gene abundance in the analysis of species and functional contribution. For RPKM, the formula is: $RPKM_i = \frac{R_i \times 10^6}{L_i \times \sum_1^n (R_j)}$, while for relative Reads Number is: $Gene_i = \frac{R_i}{\sum_1^n (R_j)}$. R_i represents the number of Reads correlated to $Gene_i$ in that sample; L_i represents nucleotide length; $\sum_1^n (R_j)$ represents the sum of reads corresponding to all genes in the sample. Based on species annotation and KEGG annotation of microbial gene set, the functions of the top 15 abundant species were analyzed at specific classification levels (kingdom, species etc.) and specific functional levels (pathway level, module, etc.) [49]. The results were visualized using an R language package.

Differences were considered significant when $P < 0.05$ and extremely significant when $P < 0.01$.

Funding

All experiments involving mice were performed using protocols approved by the Animal Center at the Eye & ENT Hospital, Fudan University (2022076).

CRediT authorship contribution statement

Hui-ying Huang: Conceptualization, Methodology, Formal analysis, Writing – original draft, Writing – review & editing. **Fei-ran Li:** Resources, Methodology, Investigation, Data curation, Writing – review & editing. **Yi-fan Zhang:** Methodology, Investigation, Formal analysis. **Hui-Ching Lau:** Conceptualization, Formal analysis. **Chi-Yao Hsueh:** Conceptualization, Data curation, Funding acquisition, Writing – review & editing. **Liang Zhou:** Visualization, Investigation, Writing – review & editing. **Ming Zhang:** Supervision, Conceptualization, Writing – review & editing, Funding acquisition.

Declaration of Competing Interest

The authors declare that they have no known competing financial interests or personal relationships that could have appeared to influence the work reported in this paper.

Data Availability

The raw data supporting the conclusions of this article has been uploaded to NCBI (PRJNA979918), without undue reservation.

Acknowledgments

This study was supported by the Natural Science Foundation of Shanghai (No. 21ZR1411900), National Natural Science Foundation of China (No. 82273097 and No. 82203727), Shanghai Sailing Program (22YF1405700) and Shanghai Municipal Key Clinical Specialty (No. shslczdzk00801).

Author contribution

Hui-ying Huang, Chi-Yao Hsueh and Ming Zhang conceived and designed the study. Hui-ying Huang, Fei-ran Li and Yi-fan Zhang constructed the animal models and collected samples. Hui-ying Huang, Fei-ran Li and Chi-Yao Hsueh analyzed the statistical data. Hui-ying Huang, Ming Zhang and Ming Zhang completed the final draft of the manuscript. All authors reviewed and approved the manuscript.

Appendix A. Supporting information

Supplementary data associated with this article can be found in the online version at doi:10.1016/j.csbj.2023.12.022.

References

- [1] Giraldi L, Leoncini E, Pastorino R, Wunsch-Filho V, de Carvalho M, et al. Alcohol and cigarette consumption predict mortality in patients with head and neck cancer: a pooled analysis within the International Head and Neck Cancer Epidemiology (INHANCE) Consortium. *Ann Oncol* 2017;28(11):2843–51. <https://doi.org/10.1093/annonc/mdx486>.
- [2] Praud D, Rota M, Rehm J, Shield K, Zatonski W, et al. Cancer incidence and mortality attributable to alcohol consumption. *Int J Cancer* 2016;138(6):1380–7. <https://doi.org/10.1002/ijc.29890>.
- [3] Huang HY, Lau HC, Ji MY, Hsueh CY, Zhang M. Association between alcohol dehydrogenase polymorphisms and the recurrence of laryngeal carcinoma. *Laryngoscope* 2022;132(11):2169–76. <https://doi.org/10.1002/lary.30083>.
- [4] Albano E. Alcohol, oxidative stress and free radical damage. *Proc Nutr Soc* 2006;65(3):278–90. <https://doi.org/10.1079/pns2006496>.
- [5] Seitz HK, Stickel F. Molecular mechanisms of alcohol-mediated carcinogenesis. *Nat Rev Cancer* 2007;7(8):599–612. <https://doi.org/10.1038/nrc2191>.
- [6] Stornetta A, Guidolin V, Balbo S. Alcohol-derived acetaldehyde exposure in the oral cavity. *Cancers* 2018;10(1). <https://doi.org/10.3390/cancers10010020>.
- [7] Cao Y, Willett WC, Rimm EB, Stampfer MJ, Giovannucci EL. Light to moderate intake of alcohol, drinking patterns, and risk of cancer: results from two prospective US cohort studies. *BMJ* 2015;351:h4238. <https://doi.org/10.1136/bmj.h4238>.
- [8] Chang JS, Lo HI, Wong TY, Huang CC, Lee WT, et al. Investigating the association between oral hygiene and head and neck cancer. *Oral Oncol* 2013;49(10):1010–7. <https://doi.org/10.1016/j.oraloncology.2013.07.004>.
- [9] Perera M, Al-Hebshi NN, Perera I, Ipe D, Ulett GC, et al. Inflammatory bacteriome and oral squamous cell carcinoma. *J Dent Res* 2018;97(6):725–32. <https://doi.org/10.1177/0022034518767118>.
- [10] Yuwanati M, Sarode SC, Gadail A, Gondivkar S, Sarode GS. Alcohol attributed Oral Cancer and Oral microbiome: emerging yet neglected research domain. *Oral Oncol* 2021;123:105596. <https://doi.org/10.1016/j.oraloncology.2021.105596>.
- [11] O'Grady I, Anderson A, O'Sullivan J. The interplay of the oral microbiome and alcohol consumption in oral squamous cell carcinomas. *Oral Oncol* 2020;110:105011. <https://doi.org/10.1016/j.oraloncology.2020.105011>.
- [12] Healy CM, Moran GP. The microbiome and oral cancer: more questions than answers. *Oral Oncol* 2019;89:30–3. <https://doi.org/10.1016/j.oraloncology.2018.12.003>.
- [13] Hsiao JR, Chang CC, Lee WT, Huang CC, Ou CY, et al. The interplay between oral microbiome, lifestyle factors and genetic polymorphisms in the risk of oral squamous cell carcinoma. *Carcinogenesis* 2018;39(6):778–87. <https://doi.org/10.1093/carcin/bgy053>.

- [14] Fan X, Peters BA, Jacobs EJ, Gapstur SM, Purdue MP, et al. Drinking alcohol is associated with variation in the human oral microbiome in a large study of American adults. *Microbiome* 2018;6(1):59. <https://doi.org/10.1186/s40168-018-0448-x>.
- [15] Hsueh CY, Huang Q, Gong H, Shen Y, Sun J, et al. A positive feed-forward loop between *Fusobacterium nucleatum* and ethanol metabolism reprogramming drives laryngeal cancer progression and metastasis. *iScience* 2022;25(2):103829. <https://doi.org/10.1016/j.isci.2022.103829>.
- [16] Lau HC, Shen Y, Huang H, Yuan X, Ji M, et al. Cross-comparison of microbiota in the oropharynx, hypopharyngeal squamous cell carcinoma and their adjacent tissues through quantitative microbiome profiling. *J Oral Microbiol* 2022;14(1):2073860. <https://doi.org/10.1080/20002297.2022.2073860>.
- [17] Gong HL, Shi Y, Zhou L, Wu CP, Cao PY, et al. The composition of microbiome in larynx and the throat biodiversity between laryngeal squamous cell carcinoma patients and control population. *PLoS One* 2013;8(6):e66476. <https://doi.org/10.1371/journal.pone.0066476>.
- [18] Gong H, Shi Y, Zhou X, Wu C, Cao P, et al. Microbiota in the throat and risk factors for laryngeal carcinoma. *Appl Environ Microbiol* 2014;80(23):7356–63. <https://doi.org/10.1128/AEM.02329-14>.
- [19] Gong H, Shi Y, Xiao X, Cao P, Wu C, et al. Alterations of microbiota structure in the larynx relevant to laryngeal carcinoma. *Sci Rep* 2017;7(1):5507. <https://doi.org/10.1038/s41598-017-05576-7>.
- [20] Hsueh CY, Gong H, Cong N, Sun J, Lau HC, et al. Throat microbial community structure and functional changes in postsurgery laryngeal carcinoma patients. *Appl Environ Microbiol* 2020;86(24). <https://doi.org/10.1128/AEM.01849-20>.
- [21] Sepich-Poore GD, Zitvogel L, Straussman R, Hasty J, Wargo JA, et al. The microbiome and human cancer. *Science* 2021;371(6536). <https://doi.org/10.1126/science.abc4552>.
- [22] Homann N, Jousimies-Somer H, Jokelainen K, Heine R, Salaspuro M. High acetaldehyde levels in saliva after ethanol consumption: methodological aspects and pathogenetic implications. *Carcinogenesis* 1997;18(9):1739–43. <https://doi.org/10.1093/carcin/18.9.1739>.
- [23] Muto M, Hitomi Y, Ohtsu A, Shimada H, Kashiwase Y, et al. Acetaldehyde production by non-pathogenic *Neisseria* in human oral microflora: implications for carcinogenesis in upper aerodigestive tract. *Int J Cancer* 2000;88(3):342–50.
- [24] Yokoyama S, Takeuchi K, Shibata Y, Kageyama S, Matsumi R, et al. Characterization of oral microbiota and acetaldehyde production. *J Oral Microbiol* 2018;10(1):1492316. <https://doi.org/10.1080/20002297.2018.1492316>.
- [25] Silva-García O, Valdez-Alarcon JJ, Baizabal-Aguirre VM. **Wnt/beta-catenin signaling as a molecular target by pathogenic bacteria.** *Front Immunol* 2019;10:2135. <https://doi.org/10.3389/fimmu.2019.02135>.
- [26] Wang J, Lu R, Fu X, Dan Z, Zhang YG, et al. Novel regulatory roles of wnt1 in infection-associated colorectal cancer. *Neoplasia* 2018;20(5):499–509. <https://doi.org/10.1016/j.neo.2018.03.001>.
- [27] Kaimala S, Al-Sbiei A, Cabral-Marques O, Fernandez-Cabezudo MJ, Al-Ramadi BK. Attenuated bacteria as immunotherapeutic tools for cancer treatment. *Front Oncol* 2018;8:136. <https://doi.org/10.3389/fonc.2018.00136>.
- [28] Becerra-Baez EI, Meza-Toledo SE, Munoz-Lopez P, Flores-Martinez LF, Fraga-Perez K, et al. Recombinant attenuated salmonella enterica as a delivery system of heterologous molecules in cancer therapy. *Cancers* 2022;14(17). <https://doi.org/10.3390/cancers14174224>.
- [29] Kung YJ, Lam B, Tseng SH, MacDonald A, Tu HF, et al. Localization of Salmonella and albumin-IL-2 to the tumor microenvironment augments anticancer T cell immunity. *J Biomed Sci* 2022;29(1):57. <https://doi.org/10.1186/s12929-022-00841-y>.
- [30] Aubry A, Mougari F, Reibel F, Cambau E. *Mycobacterium marinum*. *Microbiol Spectr* 2017;5(2). <https://doi.org/10.1128/microbiolspec.TNMI7-0038-2016>.
- [31] Sann KZ, Vissicelli NC, Bryson AL, Doern C, Mochel MC, et al. Diffuse skin nodules in an oyster farmer: disseminated *Mycobacterium marinum*. *Am J Med* 2021;134(1):e57–9. <https://doi.org/10.1016/j.amjmed.2020.06.024>.
- [32] Liu J, Yao Q, Cheng W, Ren H, Hu W. *Mycobacterium marinum* infection on both hands masquerading as eczema. *Am J Med* 2022. <https://doi.org/10.1016/j.amjmed.2022.09.002>.
- [33] Berg RD, Levitt S, O'Sullivan MP, O'Leary SM, Cambier CJ, et al. Lysosomal disorders drive susceptibility to tuberculosis by compromising macrophage migration. *Cell* 2016;165(1):139–52. <https://doi.org/10.1016/j.cell.2016.02.034>.
- [34] Pagan AJ, Yang CT, Cameron J, Swaim LE, Ellett F, et al. Myeloid growth factors promote resistance to mycobacterial infection by curtailing granuloma necrosis through macrophage replenishment. *Cell Host Microbe* 2015;18(1):15–26. <https://doi.org/10.1016/j.chom.2015.06.008>.
- [35] Badal D, Jayarani AV, Kollaran MA, Prakash D, P M, et al. Foraging signals promote swarming in starving *Pseudomonas aeruginosa*. *mBio* 2021;12(5):e0203321. <https://doi.org/10.1128/mBio.02033-21>.
- [36] Crocker AW, Harty CE, Hammond JH, Willger SD, Salazar P, et al. *Pseudomonas aeruginosa* ethanol oxidation by *AdhA* in low-oxygen environments. *J Bacteriol* 2019;201(23). <https://doi.org/10.1128/JB.00393-19>.
- [37] Chen AI, Dolben EF, Okegbe C, Harty CE, Golub Y, et al. *Candida albicans* ethanol stimulates *Pseudomonas aeruginosa* WspR-controlled biofilm formation as part of a cyclic relationship involving phenazines. *PLoS Pathog* 2014;10(10):e1004480. <https://doi.org/10.1371/journal.ppat.1004480>.
- [38] Glorieux C, Calderon PB. Catalase, a remarkable enzyme: targeting the oldest antioxidant enzyme to find a new cancer treatment approach. *Biol Chem* 2017;398(10):1095–108. <https://doi.org/10.1515/hsz-2017-0131>.
- [39] Kim HS, Lee TB, Choi CH. Down-regulation of catalase gene expression in the doxorubicin-resistant AML subline AML-2/DX100. *Biochem Biophys Res Commun* 2001;281(1):109–14. <https://doi.org/10.1006/bbrc.2001.4324>.
- [40] Akman SA, Forrest G, Chu FF, Esworthy RS, Doroshov JH. Antioxidant and xenobiotic-metabolizing enzyme gene expression in doxorubicin-resistant MCF-7 breast cancer cells. *Cancer Res* 1990;50(5):1397–402.
- [41] Deichman GI. Natural selection and early changes of phenotype of tumor cells in vivo: acquisition of new defense mechanisms. *Biochem (Mosc)* 2000;65(1):78–94.
- [42] Deichman GI. Early phenotypic changes of in vitro transformed cells during in vivo progression: possible role of the host innate immunity. *Semin Cancer Biol* 2002;12(4):317–26. [https://doi.org/10.1016/s1044-579x\(02\)00018-4](https://doi.org/10.1016/s1044-579x(02)00018-4).
- [43] Li D, Liu CM, Luo R, Sadakane K, Lam TW. MEGAHIT: an ultra-fast single-node solution for large and complex metagenomics assembly via succinct de Bruijn graph. *Bioinformatics* 2015;31(10):1674–6. <https://doi.org/10.1093/bioinformatics/btv033>.
- [44] Noguchi H, Park J, Takagi T. MetaGene: prokaryotic gene finding from environmental genome shotgun sequences. *Nucleic Acids Res* 2006;34(19):5623–30. <https://doi.org/10.1093/nar/gkl723>.
- [45] Fu L, Niu B, Zhu Z, Wu S, Li W. CD-HIT: accelerated for clustering the next-generation sequencing data. *Bioinformatics* 2012;28(23):3150–2. <https://doi.org/10.1093/bioinformatics/bts565>.
- [46] Li R, Yu C, Li Y, Lam TW, Yiu SM, et al. SOAP2: an improved ultrafast tool for short read alignment. *Bioinformatics* 2009;25(15):1966–7. <https://doi.org/10.1093/bioinformatics/btp336>.
- [47] Altschul SF, Madden TL, Schaffer AA, Zhang J, Zhang Z, et al. Gapped BLAST and PSI-BLAST: a new generation of protein database search programs. *Nucleic Acids Res* 1997;25(17):3389–402. <https://doi.org/10.1093/nar/25.17.3389>.
- [48] Xie C, Mao X, Huang J, Ding Y, Wu J, et al. KOBAS 2.0: a web server for annotation and identification of enriched pathways and diseases. *Nucleic Acids Res* 2011;39(Web Server issue):W316–322. <https://doi.org/10.1093/nar/gkr483>.
- [49] Tanca A, Abbondio M, Palomba A, Fraumene C, Manghina V, et al. Potential and active functions in the gut microbiota of a healthy human cohort. *Microbiome* 2017;5(1):79. <https://doi.org/10.1186/s40168-017-0293-3>.